

Design Methodologies for Optimizing the Electrical and Mechanical Performances of Evanescent Mode Ridge Waveguide Filters

P. Soto^a, D. de Llanos^a, V. E. Boria^a, E. Tarín^a, S. Cogollos^a, M. Taroncher^a, B. Gimeno^b

^a Instituto de Telecomunicaciones y Aplicaciones Multimedia, Universidad Politécnica de Valencia, 8G Building - access D - Camino de Vera s/n - 46022 Valencia (Spain)

^b Instituto de Ciencias de los Materiales, Universidad de Valencia, Dr. Moliner, 50 - 46100 Burjassot, Valencia (Spain)

Corresponding author: pabsopac@dcom.upv.es

Abstract

In this paper, the trade-offs between out-of-band performance, filter length, power-handling capability and insertion loss of both symmetric and asymmetric evanescent mode ridge rectangular waveguide filters are investigated. As a result, clear design methodologies for optimizing such performances are proposed. The developed methodologies are then applied to design several evanescent-mode filters, and a complete performance analysis of the symmetric and asymmetric structures is performed. From the performance analysis results, the designer can choose the more appropriate filter topology and design strategy to satisfy the prescribed set of specifications.

Keywords: Waveguide Filters, Design Methodology, Computer-Aided Design, Modal Methods, Ridge Waveguide, Bandpass Filters, Losses, Microwave Power Transmission

1. Introduction

Design requirements for passive waveguide filters in modern telecommunication systems for both space and terrestrial applications are becoming more and more restrictive. Low insertion loss, compact size, high skirt selectivity, wide spurious-free stopband and suitable power-handling capability are usually required [1]. These increasing demands have stimulated the advent and refinement of different types of filters during the last decades [2, 3]. The designer must choose a suitable filter class and topol-

ogy, and appropriately design it to obtain the best performance trade-off in order to fulfill the specifications.

Evanescent mode ridge waveguide filters, originally proposed in [4, 5] and refined in [6], exhibit many attractive features. They provide an excellent out-of-band performance with an inherent wide stopband and sharp selectivity. In addition, they are very compact in comparison with other waveguide filter types. The foremost weaknesses come from insertion loss and power considerations due to their small size. Although they benefit from the excellent insertion loss and power-handling capability innate to waveguide technology, and they have reasonable figures in these parameters in comparison with other waveguide filter types [1], evanescent mode ridge filters cannot rival with above-cutoff rectangular and circular waveguide cavity filters. As a result, they are not well-suited to implement narrowband channel filters where a high quality factor Q is required. Nevertheless, evanescent mode ridge waveguide filters are a suitable choice for moderate and wideband filters when compact size and excellent out-of-band response are involved. For instance, they can be used as preselector filters in input and output multiplexers, particularly in satellite applications where size is a major concern.

A high research effort has been devoted during the past in order to improve and take profit of the excellent properties of evanescent mode ridge filters. They have been used to obtain all-pole bandpass and quasi-lowpass responses of almost any width [7, 8]. Novel configurations

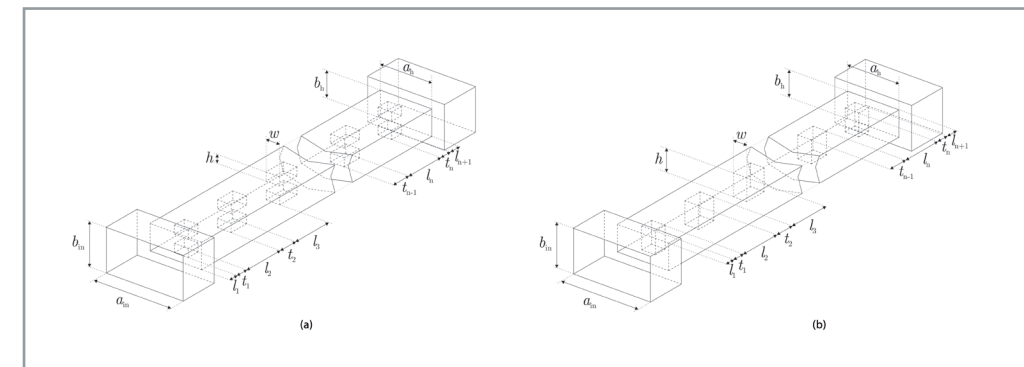


Figure 1. Symmetric in (a) and asymmetric in (b) evanescent mode ridge waveguide filter topologies under consideration, and significant physical dimensions.

have recently been presented to implement transmission zeros that further improve the skirt selectivity [9]. On the other hand, a wide range of topological variations have been proposed to improve a particular filter feature, mainly the stopband extent [10]-[12] and/or the filter total length [13, 14]. But in most cases, the improvement in these features is obtained by sacrificing insertion loss and power-handling capabilities, and usually requires harder and more expensive manufacture procedures. In [15] different ridge configurations in rectangular and circular waveguides are compared with regard to the fundamental mode attenuation coefficient and maximum transversal electric field. Nonetheless, this study has been carried out considering only the cross-section of the ridge waveguide and therefore cannot take into account effects related to the filtering structure (for instance, the ridge lengths, the field distribution along the resonators or the reactive field in the close region to the ridges).

In spite of the great practical interest of these types of structures, there is a lack of studies on its balance between insertion loss, power-handling, stopband performance and filter length. A preliminary study has been recently presented in [16], focused on symmetric ridge waveguide filters. In this paper we perform a more detailed performance analysis, thus clearer design strategies will be proposed. Additionally, the asymmetric configuration is considered and compared with the symmetric one. From this paper, the designer can identify the more appropriate filter topology (symmetric or asymmetric) as well as the design strategy to satisfy the prescribed set of electrical and mechanical filter specifications.

2. Structure Description. Analysis and Design Techniques

In waveguide technology, an evanescent mode filter is implemented in a hollow below cut-off waveguide commonly referred to as housing, which is ended with standard propagating waveguide access ports. The energy transmission between both ports is accomplished by

inserting shunt capacitive elements through the housing. The below cut-off waveguide sections spacing the capacitive elements can be modeled as impedance inverters with free shunt inductances. The inserted shunt capacitances combined with the free shunt inductances of the non-propagating housing sections provide the filter resonances, obtaining a bandpass behavior for the whole structure [5].

This paper is focused on conventional rectangular waveguide evanescent mode filters with rectangular cross-section metal inserts as capacitive elements (see Fig. 1). The centered symmetric configuration shown in Fig. 1a, with ridges in both the upper and the lower housing walls, as well as the centered asymmetric configuration, with ridges only in the upper wall (see Fig. 1b), will be considered and compared in order to establish the more appropriate one to refine each filter performance. For the sake of simplicity in the parametric analysis of the structure, all the metal inserts or ridges are considered to be centered and to have the same width w and height h . In addition, the housing width a_h and height b_h are kept constant throughout all the structure.

Since the evanescent mode filters under consideration can be easily decomposed into uniform waveguide sections and planar waveguide discontinuities, the accuracy and efficiency of modal analysis methods can be exploited [17]. To obtain the modal spectrum of the ridge waveguides, an implementation of the BI-RME method has been used [18]. The structure design is performed by the systematic decomposition procedure proposed in [19]. To compute the losses and the electric field of the designed filter, the Ansoft HFSS simulator has been used [20].

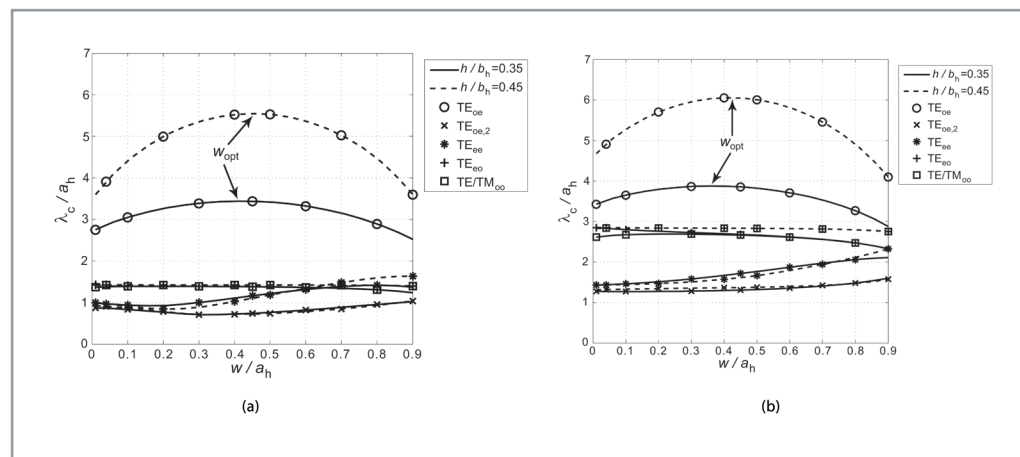
3. Parametric Analysis

To design an evanescent mode filter, a design parameter for each resonator and impedance inverter is required in order to recover an all-pole ideal response in the passband. These roles have been assigned to the ridge waveguide section lengths l_i and the below-cutoff waveguide sec-

tion lengths l_i (see Fig. 1), respectively. A modification to these parameters does not require recomputing the waveguide modes, and hence the filter design procedure is sped up. As a result, the housing dimensions a_h, b_h and the ridge height h and width w are free design parameters that must be previously fixed. They should be used to obtain the trade-off between insertion loss, power-handling, length and out-of-band performance required by the filter design specifications.

A parametric analysis has been carried out to find out the effect of such free design parameters in the filter performances. An ideal 2-pole Chebyshev bandpass transfer function centered at 7 GHz, with 280 MHz bandwidth and 15 dB return loss has been chosen as reference response. First, an evanescent mode waveguide filter with WR137 standard waveguide access ports has been designed to obtain this response. Then, the structure free design parameters have been modified over a wide range, taking into account manufacture constraints. For each value set, the reference response was recovered by using the resonator and housing section lengths l_i and t_i . The resulting filter is evaluated in terms of length, spurious-free band, insertion loss and power-handling capability. As a result, several tables and graphs relating the free design parameters and the filter performances have been obtained.

In addition, the modal spectrum of the ridge waveguides has also been characterized. As shown in Fig. 2, an increase in the ridge depth h reduces the fundamental mode cutoff frequency, whereas the cutoff frequencies of the other plotted modes are hardly changed. Therefore, the monomode operating region is increased. Concerning the ridge width w , a parabolic variation is observed in the fundamental mode cut-off wavelength, with a maximum value at $w = w_{opt}$, which is around $0.35a_h \sim 0.45a_h$ depending on the housing width to height ratio a_h/b_h . The cutoff frequencies of the higher-order modes



■ **Figure 2.** Normalized cutoff wavenumbers for double-ridge waveguides in terms of w/a_h and h/b_h . Case $a_h = 1.4b_h$ in (a) and $a_h = 0.7b_h$ in (b). The first mode of each symmetry class (even(e)/odd(o)) and the second mode of the TE_{10} -like symmetry class, $TE_{0e,2}$ are plotted.

collected in Fig. 2 are also very important for the filter performances, particularly the out-of-band response. The dimensions of the filters designed in section 5 reveal that Fig. 2a is the typical modal chart to be used for the ridges of symmetric evanescent mode filters. On the contrary, Fig. 2b shows to be very appropriate for the asymmetric filter ridge choice, since the asymmetric ridge modal spectrum can be extracted from the spectrum of a symmetric double-ridge waveguide with double height and the same w, h and a_h .

The next subsections describe the main conclusions of the parametric analysis carried out for each particular performance.

3.1 Insertion Loss

Assuming vacuum for the dielectric material, the filter losses are only due to conductor ohmic losses. For waveguide filters with good conductors, nonetheless, the losses are very low and their computation is not a simple task. The effect of the return loss ripple in the insertion loss can be significant, and it can hide small variations due to the ohmic losses required to extract the parametric analysis data. To overcome these difficulties, a metal conductor with moderate conductivity has been considered, and the deviations caused by $S_{11} \neq 0$ are compensated by considering the following modified insertion loss figure:

$$I.L.(\text{dB}) = -10 \log_{10}(|S_{11}|^2 + |S_{21}|^2) \quad [1]$$

which represents the ratio of the total input power to the power not dissipated inside the filter. Finally, to obtain a more realistic value, this figure is scaled to copper conductors by correcting the material conductivity factor.

Concerning the ridge width, the parametric analysis for both symmetric and asymmetric configurations reveals that the losses increase is

negligible for $w < 0.5w_{opt}$ and a dramatic increase is observed for $w > 0.65w_{opt}$ (see Fig. 3a and 3c). To reduce the insertion loss it is highly recommended to keep $w < 0.65w_{opt}$.

Losses also rise with the ridge depth h , and their change rate increases with the housing height (see Fig. 3b and 3d). As a result, the effect of the ridge depth h in the insertion loss figure is more important for asymmetric filters. From an insertion loss point of view, particularly for asymmetric filters, a small value of h should be chosen.

The free design parameter with the greatest influence in the filter insertion loss is the housing width a_h . As expected, a wider housing provides lower losses in both symmetric and asymmetric configurations. To optimize losses it is of paramount importance to take the wider housing that allows to satisfy the remaining filter specifications. The housing height b_h , on the other hand, is not relevant provided that the housing is high enough (especially in symmetric filters). Anyway, in order to reduce the filter losses a higher housing height normally proves to be more appropriate.

3.2 Power-Handling Capability

In payload microwave passive devices, the power handling capability is usually restricted by the dielectric breakdown electric field, as well as by

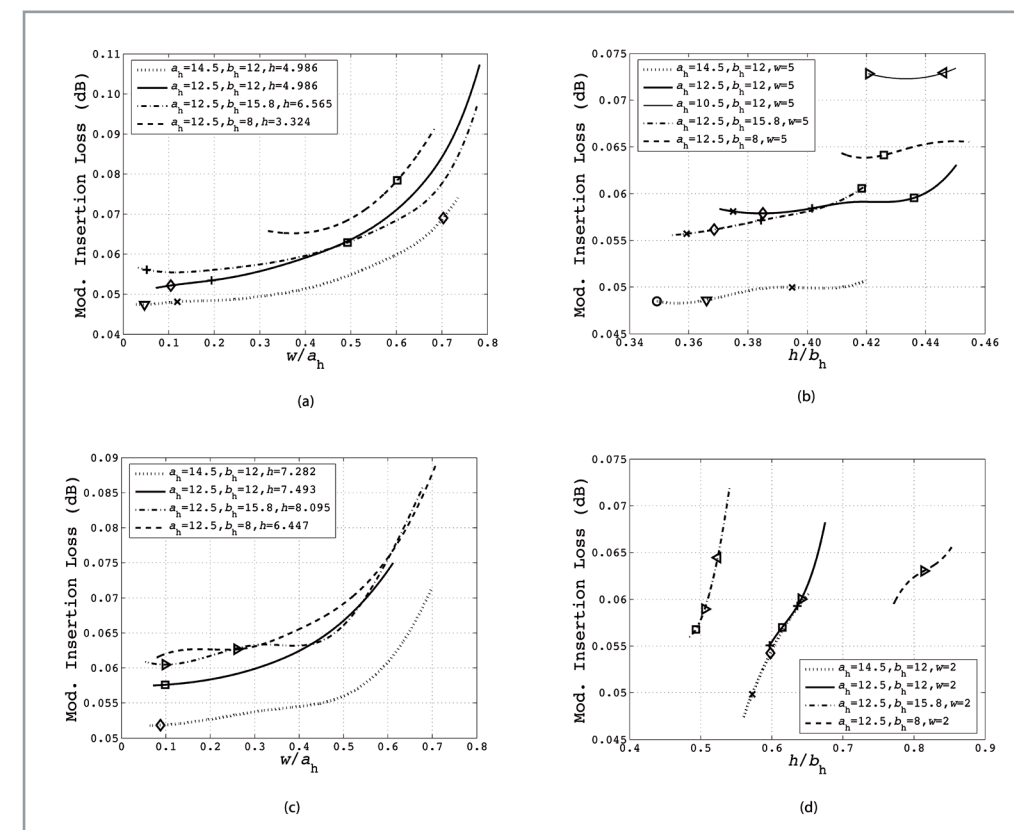
the multipactor effect under the extremely low pressure conditions in space missions. Hence, to derive the power-handling capability, the maximum electric field inside the filter has been computed for a 1W input excitation. From this value, the maximum power at the filter input to avoid dielectric breakdown and multipactor can be computed [15, 21].

The results of the parametric analysis, not shown for the sake of space, reveal that the maximum electric field depends exponentially on the ridge waveguide gap g ($g = b_h - 2h$ for symmetric filters and $g = b_h - h$ for the asymmetric configuration). Therefore, the filter power-handling capability is maximized by increasing the housing height b_h and by reducing the ridge depth h for a b_h set. A wider housing is thus preferred since it allows to use less deep ridges, and the ridge gap can be increased. Moreover, E_{max} can be slightly reduced by means of a wider ridge. Finally, asymmetric filters can provide higher ridge gaps and therefore withstands higher input power levels.

3.3 Filter Length

The filter length information has been summarized in Fig. 3 through marks. For usual filter dimensions, the inverter (i.e. housing section between ridges) lengths are the main part of the filter length. Although a wider housing provides shorter resonators as the ridge cut-off frequency

The maximum electric field depends exponentially on the ridge waveguide gap



■ **Figure 3.** Modified insertion loss for copper symmetric evanescent mode filters (in (a),(b)) and for copper asymmetric evanescent mode filters (in (c),(d)) in terms of the structure free design parameters w, h, a_h and b_h . Marks represent housing length ($\triangleleft=15$ mm, $\triangleright=17.5$ mm, $\square=20$ mm, $+=22.5$ mm, $+ =25$ mm, $\diamond=27.5$ mm, $\times=30$ mm; $\circ=32.5$ mm). All legend dimensions in mm.

The two pair of strategies obtained have the opposite interest regarding the housing width and the ridge height

is decreased, the inverter lengths are dramatically increased because the evanescent TE_{10} mode approaches cut-off and longer housing sections are required to implement the same coupling. The global result is a significant filter enlargement. Hence, a narrower housing must be taken to reduce the filter length.

The remaining free design parameters are less important than the housing width to the total filter length. Anyway, a higher housing height should be chosen to obtain a shorter structure. Regarding the ridge dimensions, to reduce the filter length it is convenient to increase the ridge width w (up to w_{opt} since for $w > w_{opt}$ the filter length reduction is insignificant) and then increase their depth h .

3.4 Spurious-free Stopband Response

Several factors can produce a first spurious response before the upper frequency of the requested stopband, f_u . The first factor arises from the propagation and resonance of the TE_{10} mode in the housing rectangular waveguide. The avoidance of this resonance restricts the maximum housing width a_h to:

$$a_h \leq a_{h,max} = (1+x) \frac{c}{2f_u} \quad [2]$$

where x is a term which takes into account that the housing sections resonate at the frequency where their lengths become approximately $\lambda_g/2$, instead of at the TE_{10} cutoff frequency.

The second resonance of the ridge sections is another effect that can end the filter stopband. This TE_{102} resonance comes from the periodic response of the resonators, and can be controlled by a suitable choice of the ridge dimensions w and h to keep the ridge length under $\lambda_g/2$ in the filter stopband.

The higher order modes are the last factor that must be considered to satisfy the stopband specification. These modes can provide an unwanted bridge to transfer energy along the structure ridge and housing sections. Using modal charts similar to Fig. 2, suitable ridge dimensions w and h can be chosen to avoid the propagation of higher order modes in the ridge sections before the stopband end. A very important case for evanescent mode waveguide filters is the TE_{01} -like mode. The cut-off frequency of this mode in the ridge and inverter sections coincides, causing a low-pass effect that produces spikes above their cut-off frequency. Although from symmetry considerations, the TE_{01} should not be excited, manufactured structures never hold a perfect symmetry and alignment, and as it will be shown in section 5, in practice the condition

$$b_h \leq b_{h,max} = \frac{c}{2f_u} \quad [3]$$

must limit the housing height to avoid TE_{01} related spikes.

4. Design Strategies

From the parametric analysis can be concluded that the filter performances are improved using the highest housing able to satisfy the out-of-band spec. Hence, according to (3), b_h will be always fixed to $b_{h,max}$.

To reduce the filter losses and increase its power-handling capability the widest housing must be chosen. The housing width is obtained by starting from (2) with $x = 0.15$ and increasing a_h while the length and the out-of-band specifications are fulfilled. In case that the designed filter does not satisfy these specifications, a narrower housing should be taken. To optimize the power-handling capability, the maximum ridge gap must be obtained by choosing the lower ridge depth h . This can be accomplished by setting $w \approx w_{opt}$ and then reducing h whereas the filter first inverter can be manufactured, the filter total length condition is fulfilled, and the ridge section length increase does not introduce the TE_{102} resonance inside the stopband. On the other hand, to optimize the filter insertion loss it is also recommended to take the lower ridge depth h but with the width set to $w \approx 0.65w_{opt}$ as the losses increase severely for $w > 0.65w_{opt}$. If a compromise between insertion loss and power-handling must be sought, an intermediate value for w could be taken.

The design procedures to optimize the filter length and the out-of-band response are similar. In both cases a manufactured filter with the narrowest housing must be sought. The following algorithm can be used:

1. For the housing dimensions set, take $w \approx w_{opt}$.
2. Increase the ridge depth h up to obtain the smaller ridge length that can be successfully manufactured.
3. Whereas the first inverter section can be manufactured, reduce a_h and goto 1.

This algorithm provides the shorter filter and maximizes the stopband. In case of out-of-band optimization, as the upper stopband frequency f_u is increased, the housing height must be reduced together with the housing width to avoid spurious responses from TE_{01} -like modes (see eq. (3)).

Two pair of quite similar strategies have been presented. The first pair optimizes insertion loss and power-handling capability, whilst the other pair is for filter length and out-of-band response. Both pair of strategies take the highest housing height allowed by (3) to satisfy the out-of-band specification, and a very similar value for the

ridge width w . However, they have the opposite interest regarding the housing width a_h and the ridge height h . Sometimes a suitable trade-off between these dimensions must be found to fill the filter specs.

To conclude this section, it is worth to remark that several techniques have been proposed in the literature to implement narrower housings, such as the stepped-wall approach [22] or the ridge transformer [23]. At expense of insertion loss and power-handling, these techniques can improve the filter spurious-free band and, for high order filters, they can also provide shorter structures. Although these topologies are out of the scope of this paper, most of the procedures and conclusions presented herein can be easily extended to these geometries.

5. Results

5.1 Comparative Study of Filter Topologies and Performances

To test the design strategies described in section 4 and evaluate the performance of evanescent mode ridge waveguide filters, four different filter specifications have been considered. A symmetric and an asymmetric filter have been designed to fulfill each specification, so that both filter topologies can be compared in terms of insertion losses, power-handling, length and stopband. For all the filter specifications, a 0.02 dB ripple Chebyshev bandpass response with 300

MHz bandwidth centered at 10 GHz has been considered. The filter access ports were standard WR-90 waveguides.

The first pair of filters, denoted now onward as filters A, have been designed to reduce the filter losses with a rejection greater than 40 dB in a stopband that ranges from 10.5 GHz to 17 GHz. Filters B have been optimized to improve the power-handling capability with the same stopband specification of filters A. On the other hand, the symmetric and asymmetric filters C have been designed to reduce the structure length without spurious passbands up to 20 GHz. The goal of filters D was to optimize the stopband extent.

Following the design strategies described in this paper, the four pairs of filters have been designed. Five order evanescent mode filters were required to satisfy the selectivity specification. Table 1 compares the structure dimensions and performances for each designed filter. The manufacture constraints consisted in a minimum length for the first inverter of 0.25 mm and ridge sections longer than 0.9 mm.

The insertion loss must be optimized in filters A. According to section 3.1, the wider housing satisfying the out-of-band requirements must be sought. On the other hand, for filters B, the ridge gap and therefore the power-handling capability can be improved on a small scale by choosing a slightly narrower housing. This housing

Asymmetric filters provide better insertion loss and much better power-handling capability for the same set of specifications

Parameter	Specs A		Specs B		Specs C		Specs D	
	Symm.	Asymm.	Symm.	Asymm.	Symm.	Asymm.	Symm.	Asymm.
a_h (mm)	10.550	10.650	10.250	10.400	6.000	6.500	6.790	6.940
b_h (mm)	8.815	8.815	8.815	8.815	7.490	7.490	5.275	5.400
w (mm)	2.920	2.600	4.620	4.680	2.700	2.440	3.050	2.780
h (mm)	3.200	4.750	3.020	4.600	3.506	5.650	2.480	4.652
gap (mm)	2.415	4.065	2.775	4.215	0.478	1.840	0.315	0.748
$l_1=l_6$ (mm)	3.225	3.145	2.475	2.695	0.250	0.250	0.250	0.250
$t_1=t_5$ (mm)	3.638	2.941	5.460	3.892	0.901	0.900	0.901	0.903
$l_2=l_5$ (mm)	12.600	12.235	11.045	11.185	6.610	6.035	7.785	7.685
$t_2=t_4$ (mm)	4.038	3.538	6.258	4.892	1.435	2.965	1.411	1.870
$l_3=l_4$ (mm)	14.020	13.690	12.345	12.535	7.065	6.312	8.278	8.138
t_3 (mm)	4.030	3.521	6.241	4.860	1.433	2.955	1.411	1.868
Length (mm)	79.072	74.619	81.407	75.258	33.953	35.879	38.661	39.560
$I \cdot L$ (dB)	0.2253	0.2095	0.2552	0.2574	0.4315	0.3781	0.4215	0.3817
E_{max} (V/cm)	423.56	294.39	327.87	206.21	1 899.65	438.23	2 474.26	1 045.86
Stopband (GHz)	10.4-17.0	10.4-17.0	10.4-17.0	10.4-17.0	10.4-20.0	10.4-20.0	10.4-28.4	10.4-27.4

Table 1. Symmetric and asymmetric filter dimensions and performances for the four specifications considered.

To avoid the stopband spikes that come from manufacture asymmetries, the limitation (3) should be enforced

gives the designer a margin to fulfill the stopband specs since the spurious response goes up in frequency. This margin can be invested in a ridge section length increase due to a higher ridge gap choice; resulting in better power-handling figures (compare filters A-B in Table 1).

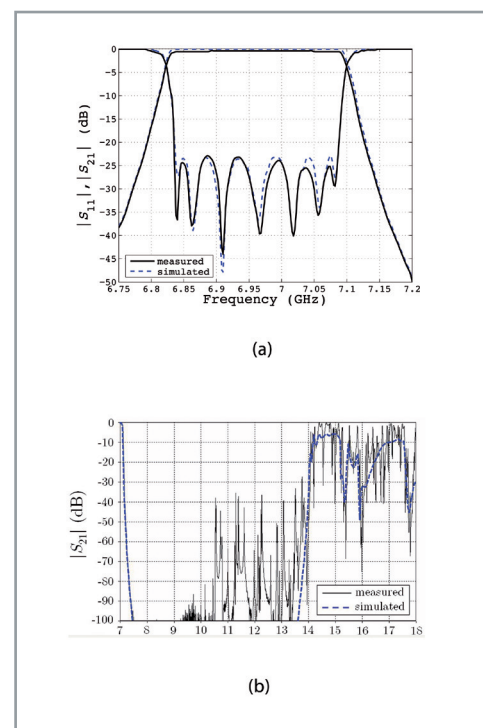
The out-of-band performance and the filter length are optimized by using a narrower housing. This housing can be obtained following the iterative algorithm described in section 4. In filters D, the increase in the stopband extent requires a lower housing height to keep the TE_{01} mode below cut-off in a wider stopband. This housing increases the step in the first structure discontinuity, thus reducing the housing section length l_1 . Hence, when the spurious-free band is optimized, a wider housing is required to be able to implement the first filter inverter and a longer filter is obtained. This is the main discrepancy in the design procedure for filters D and C (see Table 1).

With regard to the comparison between symmetric and asymmetric topologies, the asymmetric filters provide better insertion loss and much better power-handling capability for the same set of specifications. The only exception to this rule comes from the filters designed under specs B. In this case the insertion loss is almost equal because the losses increase with the ridge width w starts from a lower w in the asymmetric topologies (compare Fig. 3a and 3c). Anyway, the results in Table 1 reveal that an asymmetric evanescent mode filter can be easily designed to provide simultaneously better losses and power-handling capability than any symmetric counterpart. Even though slightly shorter filters can be obtained from symmetric configurations optimized to reduce length, for evanescent mode filters demanding good figures in insertion loss and power-handling with moderate stopband requirements the asymmetric filters are substantially shorter. As a result, the use of the symmetric topology is only recommended when an extreme optimization of the out-of-band performance or the filter length is requested in combination with poor requirements in insertion loss and power-handling capability.

5.2 Experimental Results

Two C-band evanescent mode ridge waveguide filters have been designed and manufactured to validate the design procedures proposed in this paper with real measurements. For both filters, an all-pole 249 MHz bandwidth Chebychev response centered at 6.966 GHz has been chosen. The passband return loss has been set to 22 dB. Both filters were manufactured from an aluminium block by using conventional milling techniques, and were ended with standard WR-137 ports. A silver-plated coating was applied to the metal conductor walls to reduce the ohmic losses.

The first filter was designed to optimize insertion loss with a rejection greater than 40 dB between 7.2 and 14 GHz. An asymmetric configuration

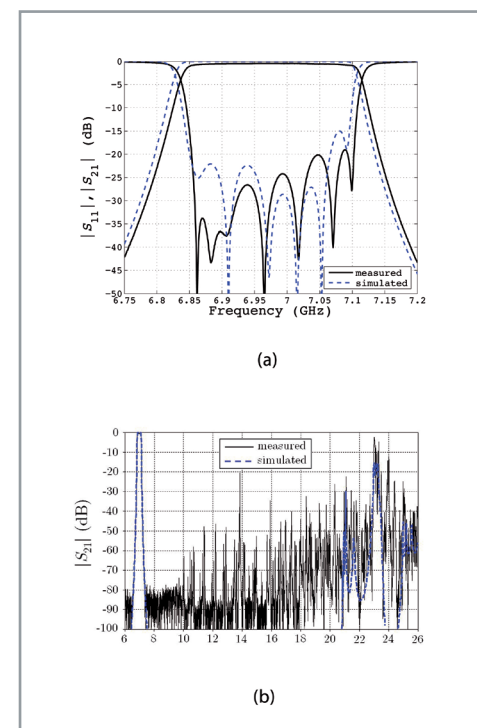


■ **Figure 4.** Comparison between simulated and measured response in the passband (a) and the stopband (b) for the manufactured asymmetric filter.

can fulfill the spurious band specifications with lower insertion loss than a symmetric topology. A 7th order filter was required to satisfy the stopband requirement at 7.2 GHz. Figure 4 depicts the simulated and measured filter responses. The physical dimensions obtained from the structure dimensional control were employed to perform the simulations. The passband measured insertion loss was 0.35 dB, which translates into a quality factor of about 3 600. The filter total length (excluding access ports) was 102.13 mm.

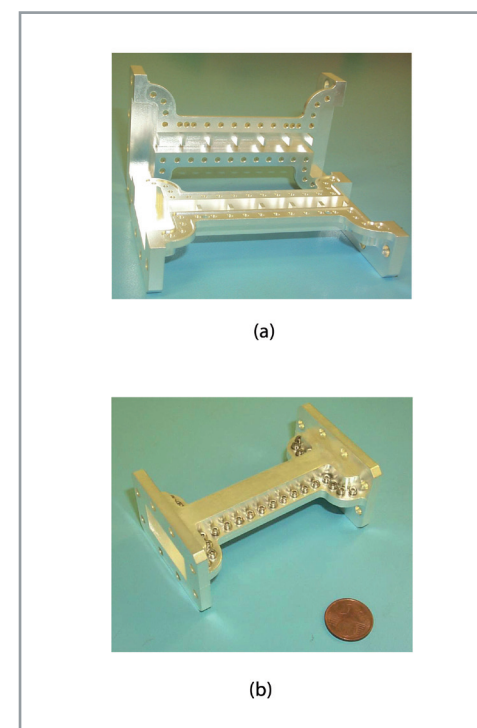
For the second filter, the design criterion was to optimize the filter length with a stopband ranging between 7.2 and 21 GHz. According to the topology comparative analysis, a symmetric configuration was taken. A filter with 7 resonators was required to fulfill the design specifications. Figure 5 compares the simulated (after dimensional control) and measured response of the manufactured filter. In Fig. 6 the pieces of the symmetric filter and the final assembled structure are shown. A very compact C-band structure of only 73.62 mm length (excluding access ports) was obtained. As it was expected, an increase in the passband insertion loss was observed. The measured insertion loss was 0.45 dB, so that the measured quality factor drops to nearly 2 800.

As shown in Fig. 4a and 5a, the agreement between the measured and the simulated bandpass response is very good, particularly for the asymmetric filter. The differences can be attributed to manufacture tolerances, whose effect is more important in the symmetric filter



■ **Figure 5.** Comparison between simulated and measured response in the passband (a) and the stopband (b) for the manufactured symmetric filter.

where the more sensitive dimension, the ridge gap, is smaller. Figures 4b and 5b show the filter stopband responses. The agreement is very good, but the measured stopband responses are plagued with very narrow spikes. For these filters the housing height constraint was not applied, since from the simulations we wrongly conclude that b_h did not affect to the out-of-band per-



■ **Figure 6.** Parts of the manufactured symmetric filter in (a) and assembled structure in (b).

formance. A higher housing was therefore taken. Nonetheless, spurious appeared in the stopband response. The authors have proved that these spurious come from asymmetries due to manufacture tolerances and assembly misalignments. These impairments excite unexpected modes (for instance, the TE_{01} mode) that theoretically should not appear in the structure under TE_{10} incidence. Such modes provide an alternative path for the power transmission along the filter, thus introducing spurious responses in the filter stopband. In fact, the first spike in both filters appears exactly at the TE_{01} cut-off frequency. To avoid these spikes, the limitation (3) should be enforced.

6. Conclusions

The performance compromises of symmetric and asymmetric evanescent mode ridge waveguide filters have been deeply investigated. As a result, clear design strategies to optimize insertion loss, power-handling, out-of-band response and length have been proposed. Using these strategies, a complete performance analysis and comparison of both symmetric and asymmetric topologies are carried out. From the methods and results presented in this paper, the designer can choose the best topology to satisfy a prescribed set of specifications. Furthermore, he can also select the design strategy to be followed in order to achieve the best performance trade-off for the evanescent mode ridge waveguide filter structure.

Acknowledgement

The authors thank Thales Alenia Space for the manufacturing and measurement of the filter prototypes.

References

- [1] J. Uher, J. Bornemann, and U. Rosenberg, Waveguide Components for Antenna Feed Systems: Theory and CAD. Artech-House, 1993.
- [2] G. L. Matthaei, L. Young, and E. M. T. Jones, Microwave Filters, Impedance-Matching Networks, and Coupling Structures. Artech-House, 1980.
- [3] R. J. Cameron, C. M. Kudsia, and R. R. Mansour, Microwave Filters for Communication Systems: Fundamentals, Design and Applications. Wiley-Interscience, 2007.
- [4] G. F. Craven, "Waveguide bandpass filters using evanescent modes", Electron. Lett., vol. 2, no. 7, pp. 251-252, 1966.
- [5] G. F. Craven and C. K. Mok, "The design of evanescent mode waveguide bandpass filters for a prescribed insertion loss characteristic", IEEE Trans. Microwave Theory Tech., vol. 19, no. 3, pp. 295-308, 1971.

- [6] R. V. Snyder, "New application of evanescent mode waveguide to filter design", *IEEE Trans. Microwave Theory Tech.*, vol. 25, no. 12, pp. 1013-1021, 1977.
- [7] A. Kirilenko, L. Rud, V. Tkachenko, and D. Kulik, "Design of band-pass lowpass evanescent-mode filters on ridged waveguides", in *Proc. 29th EuMC, Munich*, pp. 239-242, October. 1999.
- [8] Z. M. Liu, J. A. Ruiz-Cruz, W. Chi, and K. A. Zaki, "An extremely wideband ridge waveguide filter", in *2004 MTT-S Int. Microwave Symp., Fort Worth*, pp. 615-618, June. 2004.
- [9] J. A. Ruiz-Cruz, M. A. E. Sabbagh, K. A. Zaki, J. M. Rebollar, and Y. Zhang, "Canonical ridge waveguide filters in LTCC or metallic resonators", *IEEE Trans. Microwave Theory Tech.*, vol. 53, no. 1, pp. 174-182, 2005.
- [10] A. M. K. Saad, J. D. Miller, A. Mitha, and R. Brown, "Analysis of antipodal ridge waveguide structure and application on extremely wide stopband lowpass filter", in *1986 MTT-S Int. Microwave Symp., Baltimore*, pp. 361-363. 1986.
- [11] A. M. K. Saad, J. D. Miller, A. Mitha, and R. Brown, "Evanescent-mode serrated ridge waveguide bandpass harmonic filters", in *Proc. 17th EuMC, Rome*, pp. 287-291. 1986.
- [12] A. Kirilenko, L. Rud, V. Tkachenko, and D. Kulik, "Evanescent-mode ridged waveguide bandpass filters with improved performance", *IEEE Trans. Microwave Theory Tech.*, vol. 50, no. 5, pp. 1324-1327, 2002.
- [13] T. Shen and K. A. Zaki, "Length reduction of evanescent-mode ridge waveguide bandpass filters", in *2001 MTT-S Int. Microwave Symp., Phoenix*, pp. 1491-1494. June. 2001.
- [14] M. Capurso, M. Piloni and M. Guglielmi, "Resonant aperture filters: improved out-of-band rejection and size reduction", in *Proc. 31st EuMC, London*, pp. 331-334. 2001.
- [15] Y. Rong and K. A. Zaki, "Characteristics of generalized rectangular and circular ridge waveguides", *IEEE Trans. Microwave Theory Tech.*, vol. 48, no. 2, pp. 258-265, 2000.
- [16] P. Soto, D. de Llanos, E. Tarín, V. E. Boria, B. Gimeno, A. Oñoro, I. Hidalgo, and M. J. Padilla, "Efficient analysis and design strategies for evanescent mode ridge waveguide filters", in *Proc. 36th EuMC, Manchester*, pp. 1095-1098, September. 2006.
- [17] G. Conciauro, M. Guglielmi, and R. Sorrentino, *Advanced Modal Analysis*, John Wiley & Sons, 2000.
- [18] S. Cogollos, S. Marini, V. E. Boria, P. Soto, A. Vidal, H. Esteban, J. V. Morro, and B. Gimeno, "Efficient modal analysis of arbitrarily shaped waveguides composed of linear, circular, and elliptical arcs using the BI-RME method", *IEEE Trans. Microwave Theory Tech.*, vol. 51, no. 12, pp. 2378-2390, 2003.
- [19] M. Guglielmi, "Simple CAD procedure for microwave filters and multiplexers", *IEEE Trans. Microwave Theory Tech.*, vol. 42, no. 7, pp. 1347-1352, 1994.
- [20] HFSS, Ansoft Corporation, Pittsburgh.
- [21] A. J. Hatch and H. B. Williams, "Multipacting modes of high-frequency gaseous break-

down", *The Physical Review*, vol. 112, no. 3, pp. 681-685, 1958.

- [22] R. V. Snyder, "Broadband waveguide filters with wide stopbands using a stepped-wall evanescent-mode approach", in *1983 MTT-S Int. Microwave Symp., Boston*, pp. 151-153. 1983.
- [23] J. C. Nanan, J. Tao, H. Buadrand, B. Theron, and S. Vigneron, "A two-step synthesis of broadband ridged waveguide bandpass filters with improved performances", *IEEE Trans. Microwave Theory Tech.*, vol. 39, no. 12, pp. 2192-2197, 1991.

Biographies



Pablo Soto

was born in 1975 in Cartagena, Spain. He received the M.S. degree in Telecommunication Engineering from the Universidad Politécnica de Valencia in 1999, where he is currently working toward the Ph.D. degree. In 2000 he joined the Departamento de Comunicaciones, Universidad Politécnica de Valencia, where he is a Lecturer since 2002. In 2000 he was a fellow with the European Space Research and Technology Centre (ESTEC-ESA), Noordwijk, the Netherlands. His research interests comprise numerical methods for the analysis and automated design of passive waveguide components. Mr. Soto received the 2000 COIT/AEIT national award to the best Master Thesis in basic information and communication technologies.



Daniel de Llanos

was born in 1979 in Valencia, Spain. He received the M.S. degree in Telecommunication Engineering from the Universidad Politécnica de Valencia in 2003. In 2003 he joined the research group BET (Bioengineering, Electronics and Telemedicine), from the Universidad Politécnica de Valencia, working in a project sponsored by Telefónica Móviles. In 2004 he joined the company Motorola S.A, Madrid, inside the group GSM Networks, where he is currently working as UMTS UTRAN Optimization Engineer.



Vicente E. Boria

See page 17



Eva Tarín

was born in 1983 in Cheste, Spain. She received the B.S. degree and M.S. degree in Telecommunication Engineering from the Universidad Politécnica de Valencia (first-class honors) in 2005 and 2008, respectively. Since 2009 she is a secondary school teacher on mathematics in Valencia. Her research interests deals with numerical methods for the analysis and design of waveguide components. Ms. Tarín has been awarded with several awards for her outstanding academic record. She also held a 2005-2006 IEEE MTT pre-graduate scholarship.



Santiago Cogollos

was born in Valencia, Spain, on January 15, 1972. He received the degree in telecommunication engineering and the Ph. D. degree from the Polytechnic University of Valencia, Valencia, Spain, in 1996 and 2002, respectively. In 2000 he joined the Communications Department of the Polytechnic University of Valencia, where he was an Assistant Lecturer from 2000 to 2001, a Lecturer from 2001 to 2002, and became an Associate Professor in 2002. He has collaborated with the European Space Research and Technology Centre of the European Space Agency in the development of modal analysis tools for payload systems in satellites. In 2005 he held a post doctoral research position working in the area of new synthesis techniques in filter design at University of Waterloo, Waterloo, Ont., Canada. His current research interests include applied electromagnetics, mathematical methods for electromagnetic theory, analytical and numerical methods for the analysis of waveguide structures, and design of waveguide components for space applications.



Mária Taroncher

was born in Llíria, Valencia, Spain on October 8, 1979. She received the Telecommunications Engineering degree from the Universidad Politécnica de Valencia (UPV), Valencia, Spain, in 2003, and is currently

working toward the Ph.D. degree at UPV. From 2002 to 2004, she was a Fellow Researcher with the UPV. Since 2004, she has been a Technical Researcher in charge of the experimental laboratory for high power effects in waveguide devices at the Research Institute iTEAM, UPV. In 2006 she was awarded a Trainee position at the European Space Research and Technology Centre, European Space Agency (ESTEC-ESA), Noordwijk, The Netherlands, where she worked in the Payload Systems Division Laboratory in the area of Multipactor, Corona Discharge and Passive Intermodulation (PIM) effects. Her current research interests include numerical methods for the analysis of waveguide structures and the acceleration of the electromagnetic analysis methods.



Benito Gimeno

was born in Valencia, Spain, on January 29, 1964. He received the Licenciado degree in Physics in 1987 and the PhD degree in 1992, both from the Universidad de Valencia, Spain. He was a Fellow at the Universidad de Valencia from 1987 to 1990. Since 1990 he served

as Assistant Professor in the Departamento de Física Aplicada y Electromagnetismo at the Universidad de Valencia, where he became Associate Professor in 1997. His current research interests include the areas of computer-aided techniques for analysis of passive components for space applications, waveguides and cavities including dielectric objects, electromagnetic band-gap structures, frequency selective surfaces, and non-linear phenomena appearing in power microwave subsystems (multipactor and corona effects).